A structural and catalytic model for zinc phosphoesterases†

Rebecca R. Buchholz,[a] Morgan E. Etienne,[a] Anneke Dorgelo,[a] Ruth E. Mirams,[a] Sarah J. Smith,[a] Shiao Yun Chow,[a] Lyall R. Hanton,[b] Geoffrey B. Jameson,[c] Gerhard Schenk[a] and Lawrence R. Gahan*[a]

Received 24th April 2008, Accepted 4th August 2008
First published as an Advance Article on the web 23rd September 2008
DOI: 10.1039/b806391e

A structural model for the active site of phosphoesterases, enzymes that degrade organophosphate neurotoxins, has been synthesised. The ligand [2-((2-hydroxy-3-(((2-hydroxyethyl)(pyridin-2-ylmethyl)amino)methyl)-5-methylbenzyl)(pyridin-2-ylmethyl)amino)acetic acid] (H_3L1) and two Zn(II) complexes have been prepared and characterised as $[Zn_2(HL1)(CH_3COO)](PF_6)\cdot H_2O$ and $Li[Zn_2(HL1)]_4(PO_4)_2(PF_6)_3\cdot(CH_3OH)$. The ligand ($H_3L1$) and complex $[Zn_2(HL1)(CH_3COO)](PF_6)\cdot H_2O$ were characterised through ^1H NMR, ^{13}C NMR, mass spectroscopy and microanalysis. The X-ray crystal structure of $Li[Zn_2(HL1)]_4(PO_4)_2(PF_6)_3\cdot(CH_3OH)$ revealed a tetramer of dinuclear complexes, bridged by two phosphate molecules and bifurcating acetic acid arms. Functional studies of the zinc complex with the substrate bis(4-nitrophenyl)phosphate (bNPP) determined the complex with $HL1^{2-}$ to be a competent catalyst with $k_{cat} = 1.26 \pm 0.06 \times 10^{-6}$ s^{-1}.

Introduction

Phosphoesterases hydrolyse the phosphorus oxygen bond of tri-, di- or monophosphoesters.[1–4] Among them, triesterases are enzymes that have acquired the ability to degrade a range of synthetic organophosphates (OP) including chemical warfare agents such as sarin and VX, and insecticides such as paraoxon.[5,6] The members of this group of enzymes have been isolated and characterised from *Pseudomonas diminuta*, *Flavobacterium sp.* and *Agrobacterium radiobacter*.[7–10] The binuclear glycerophosphodiesterase from *Enterobacter aerogenes* (GpdQ)[11,12] is structurally unrelated to these triesterases but also has modest activity towards OPs and diester products of VX degradation.[4] Importantly, recombinant *Escherichia coli* co-expressing the triesterase from *A. radiobacter* (OpdA) and GpdQ is able to survive under conditions where OPs are the only source of phosphate.[12] Thus, this bacterial system may be sufficiently robust to find an application in the bioremediation of, for example, water supplies that are contaminated with pesticide wastes.[12]

The *in vivo* metal ion compositions of metalloenzymes are often diverse. Anomalous scattering analysis of OpdA has indicated that its likely metal ion composition is of the Fe(II)–Zn(II) type, whereas GpdQ is speculated to be of the di-Fe(II) type.[13,14] However, the catalytic activity may be regenerated from the apo-forms of both enzymes upon addition of various divalent metals, including Mn(II), Co(II), Cd(II) and Zn(II).[11,14,15] The highest hydrolytic activity for the OP-degrading hydrolase from *P. diminuta* (OPH), OpdA and GpdQ has been recorded with Co(II).[13,15,16]

OPH and OpdA have high structural similarity and sequence homology (~90% identity), and are assumed to have a similar mechanism of action.[9,10,17] The active sites of these enzymes provide essentially the same N,O asymmetric coordination environment for the two divalent metal ions (Fig. 1). The metal ions are coordinated by nitrogen donors located on four histidine ligands, an aspartate, a carboxylated lysine, and a metal ion-bridging hydroxide ion.[9,16,18–20] In GpdQ, the more buried α-metal is coordinated in a distorted trigonal-bipyramidal arrangement by the donor atoms from His197, His10, Asp8, the bridging Asp50 and hydroxide, whilst the more solvent exposed β-metal is ligated by His156, His195, Asn80 and the two bridging donors.[13]

Both kinetic studies and kinetic isotope (^{18}O) effect studies have determined that the hydrolysis of the P–O bond of OPs by phosphotriesterases is accompanied by an inversion of configuration at the phosphorus atom.[21] While this general mechanism is widely accepted, some details such as the identity of the attacking nucleophile remain subject to debate, with possibilities including the bridging hydroxo, a terminal hydroxo or activated uncoordinated water.[13,17–22] While a mechanism involving the bridging hydroxide was initially favoured, an alternative model has gained credence, whereby a hydroxide that is terminally bound to the α-metal ion attacks the phosphorus centre of the substrate, which is monodentately bound to the β-metal ion.[20]

Biomimetics are useful for a number of reasons, including that it is often easier to study structural and mechanistic features of complex biological systems using a smaller and simpler model system.[3,23–27] Models may be structural, electronic and/or functional mimics, although lower catalytic activity is to be expected from the model complexes as they tend to be poor functional mimics in comparison with their corresponding enzyme systems.[28–34] This approach is exemplified by recent investigations into the structure and function of the binuclear mono and diesterase purple acid phosphatase.[27,31,33,35] We report

[a]*School of Molecular and Microbial Sciences, The University of Queensland, Queensland, Australia 4072. E-mail: gahan@uq.edu.au*
[b]*Department of Chemistry, Te Tari Hua-Ruanuku, University of Otago, PO Box 56, Dunedin, New Zealand*
[c]*Massey University, Palmerston North Campus, Private Bag 11222, Palmerston North, 5301, New Zealand*

† Electronic supplementary information (ESI) available: TOF MS data. CCDC reference number 686253. For ESI and crystallographic data in CIF or other electronic format see DOI: 10.1039/b806391e

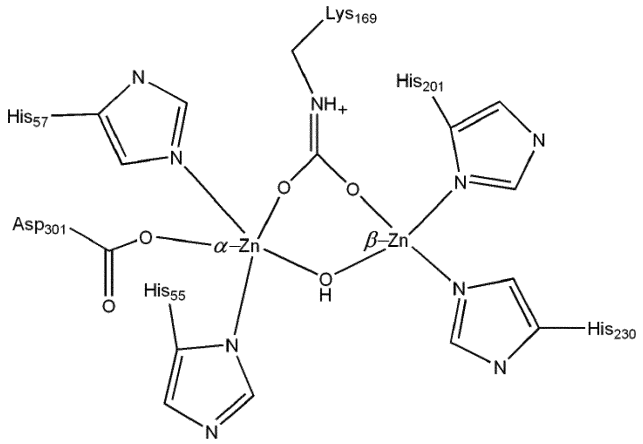

(a) OPH

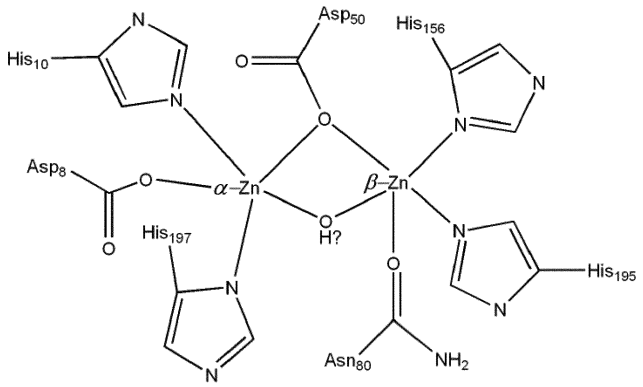

(b) GpdQ

Fig. 1 Schematic of the active sites of OPH[25] and GpdQ[13]

herein, the synthesis and characterisation of [2-((2-hydroxy-3-(((2-hydroxyethyl)(pyridin-2-ylmethyl)amino)methyl)5-methylbenzyl)(pyridin-2-yl-methyl)amino)acetic acid] (H_3L1) (Fig. 2) and its di-Zn(II) complex, specifically as a structural model for the GpdQ enzyme. The complex has been characterised spectroscopically, and its catalytic properties were investigated using the substrate bis(4-nitrophenyl) phosphate (bNPP). In addition, an octanuclear zinc(II) complex of $HL1^{2-}$ has been characterised by X-ray crystallography.

Results and discussion

Synthesis of the ligand and complex

The ethyl ester H_2EtL1 was produced in a reaction sequence (Scheme 1) involving a statistical reaction between *N*-(2-pyridylmethyl)glycine ethyl ester,[36] *N*-(2-pyridylmethyl)-2-aminoethanol[37] and 2,6-bis(chloromethyl)-4-methyl-phenol[38] in tetrahydrofuran in the presence of base. Chromatographic separation of the mixture with silica readily produced ethyl 2-((2-hydroxy-3-(((2-hydroxyethyl)(pyridin-2-ylmethyl)amino)methyl)-5-methylbenzyl)(pyridin-2-ylmethyl)amino)acetate (H_2EtL1) as well as the symmetrical analogues [diethyl 2,20-(2-hydroxy-5-methyl-1,3-phenylene)bis(methylene)bis((pyridin-2-ylmethyl)azanediyl)diacetate] and the previously reported ligand 2,6-bis([(2-pyridylmethyl)(2-hydroxyethyl)amino]methyl)-4-methylphenol (H_3L2) (Fig. 2).[28] The reaction of H_2EtL1 with lithium hydroxide resulted in a lithium salt of [2-((2-hydroxy-3-(((2-hydroxyethyl)(pyridin-2-ylmethyl)amino)methyl)-5-methylbenzyl)(pyridin-2-ylmethyl)-amino)acetic acid] (LiH_2L1).[39]

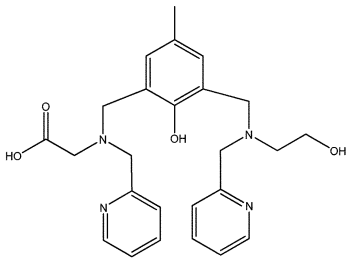

[2-((2-hydroxy-3-(((2-hydroxyethyl)(pyridin-2-ylmethyl)amino)methyl)5-methylbenzyl)(pyridin-2-yl-methyl)amino)acetic acid] (H_3L1)

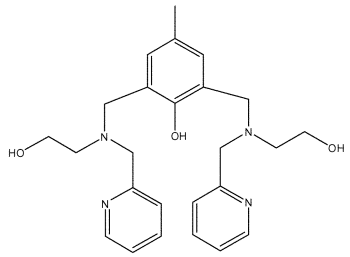

2,6-bis([(2-pyridylmethyl)(2-hydroxyethyl)amino]methyl)-4-methylphenol (H_3L2)[28]

Fig. 2 H_3L1 and H_3L2.

The nomenclature employed for the ligand refers to the number of protons possibly available for removal upon complexation. Thus, for H_3L1, the inference is that the protons on the phenoxide, the carboxylate and the pendant alcohol are candidates for deprotonation. Possible protonation sites on the pyridine nitrogen atoms are not included in this nomenclature but these are considered in the determination of the ligand pK_a values (*vide infra*).

The reaction of LiH_2L1 with zinc acetate in the presence of sodium hexafluorophosphate resulted in a white solid, for which microanalytical and spectroscopic data support the assignment as $[Zn_2(HL1)(CH_3COO)](PF_6)\cdot H_2O$. The crystal produced for the X-ray structural study was isolated from the bulk reaction mixture upon standing with sodium hexafluorophosphate. Subsequent structural analysis indicated a complex structure (*vide infra*) most likely resulting from the crystallisation methodology and not necessarily representative of the initial product produced in the reaction. The structure of this complex represents its only form of characterization and is reported because of its high nuclearity and some of its structural features.

Solid state structure

The complex $Li[Zn_2(HL1)]_4(PO_4)_2(PF_6)_3\cdot(CH_3OH)$ crystallised as a tetramer of dinuclear $[Zn_2(HL1)]^{2+}$ units with two PO_4^{3-} molecules, one lithium ion and a molecule of methanol within the complex cation. Diagrams of the complex cation are shown in Fig. 3 and Fig. 4 with the crystal data listed in Table 1 with important bond distances and angles listed in Table 2 (listed bond lengths and angles involving disordered atoms refer to the main residue, *i.e.* the higher occupancy). The two PO_4^{3-} anions are

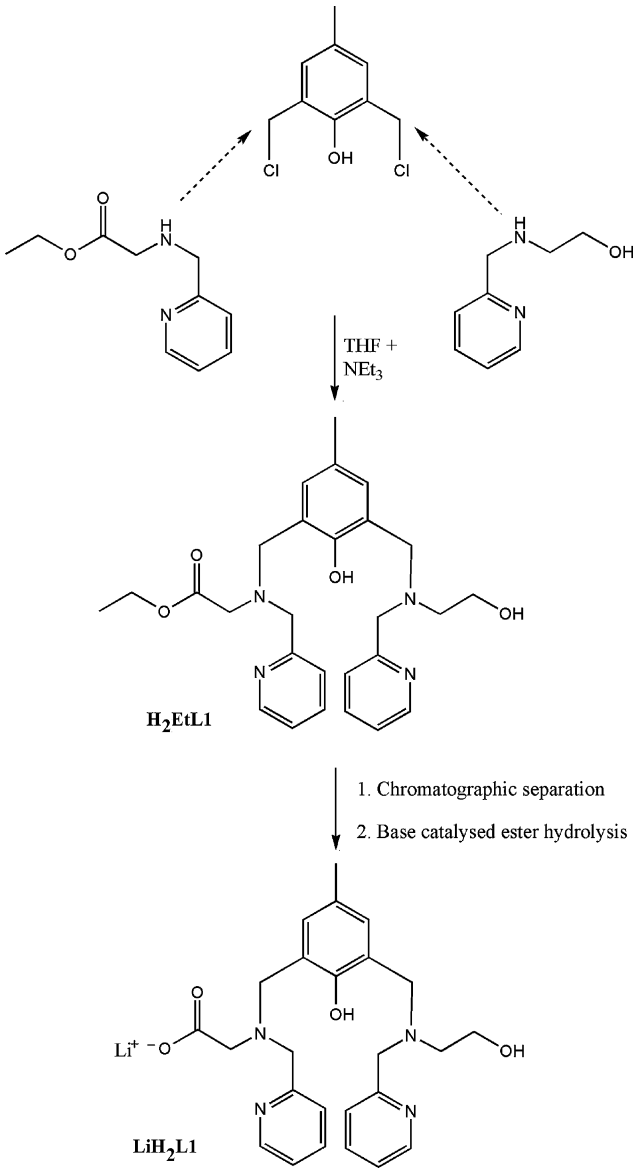

Scheme 1 Synthesis of ethyl-2-((2-hydroxy-3-(((2-hydroxyethyl)(pyridin-2-ylmethyl)amino)methyl)-5-methylbenzyl)(pyridin-2-ylmethyl)amino)-acetate (H_2EtL1) and the lithium salt (LiH_2L1)

each connected to four Zn(II) ions. Three PF_6^- anions, two of them disordered, complete the structure. A significant disorder was also observed in many of the ligand's aromatic rings. The electron density, apparent in the centre of the tetrameric structure, was assigned to a lithium ion most likely arising from the use of the lithium salt of the ligand in the synthetic step; the isotropic atomic displacement parameters suggested that either a sodium or a hydrogen ion was inappropriate. The lithium is strongly associated with the oxygen of the PO_4^{3-} anions (1.95–2.06 Å) and with the oxygen atom of a solvent methanol molecule (2.43 Å). Although no PO_4^{3-} was intentionally added to the crystallising mixture, possible sources include an impurity in the sodium hexafluorophosphate, or from hydrolysis of PF_6^- to PO_4^{3-} by the Zn(II) complex.[40] The bond lengths and angles, as well as the coordinative saturation, of this moiety support its assignment as PO_4^{3-} as opposed to $PO_2F_2^-$, another hydrolytic product of

Table 1 Crystallographic data for $Li[Zn_2(HL1)]_4(PO_4)_2(PF_6)_3\cdot(CH_3OH)$

Empirical formula	$C_{101}H_{116}F_{18}LiN_{16}O_{25}P_5Zn_8$
Formula weight	2980.85
Temperature/K	90(2)
Wavelength/Å	0.71073
Crystal system	Monoclinic
Space group	$P2_1/c$
a/Å	16.560(3)
b/Å	40.130(2)
c/Å	19.710(3)
β/°	104.92(2)
V/Å^3	12657(3)
Z	4
Absorption coefficient/mm^{-1}	1.650
D_{calcd}/Mg m^{-3}	1.564
Reflections collected/unique	80 413/19 659 ($R_{int} = 0.0414$)
Data/restraints/parameters	19 659/4700/2352
Final R indices [$I > 2\sigma(I)$]	$R = 0.0994$, w$R_2 = 0.2348$
R indices (all data)	$R = 0.1195$, w$R_2 = 0.2491$

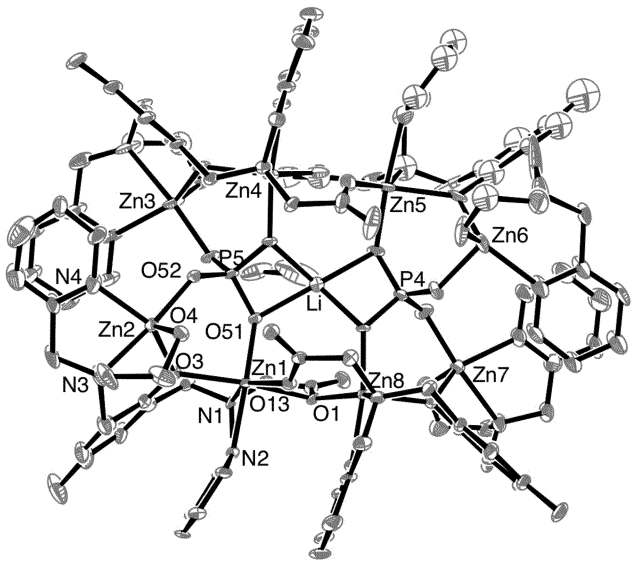

Fig. 3 ORTEP plot of the main residue of the disordered complex cation of $Li[Zn_2(HL1)]_4(PO_4)_2(PF_6)_3\cdot(CH_3OH)$. Thermal probability ellipsoids are drawn at the 50% probability level. Hydrogen atoms are omitted for clarity.

PF_6^-.[41] In $PO_2F_2^-$, the P–F and P–O bond lengths are different (P–F, 1.49–1.55 Å; P–O, 1.43–1.47 Å)[42–44] whereas in the present structure there is no difference between the two sets of bonds of the tetrahedral anions (1.509–1.541 Å). The charge balance also supports the presence of PO_4^{3-} rather than $PO_2F_2^-$.

There are four six-coordinate (Zn(1), Zn(4), Zn(5) and Zn(8)) and four five-coordinate zinc centres (Zn(2), Zn(3), Zn(6) and Zn(7)) in the complex cation. The molecule is composed of two halves, each composed of two $HL1^{2-}$ ligands coordinated to four Zn(II) ions. The halves are connected by the two PO_4^{3-} anions, separating the zinc atoms by approximately 4.72 Å, and forming a zipper-like connection with the Li^+ cation in the centre of the structure, but not present on a symmetry element. One side of the zipper is composed of Zn(7), Zn(8), Zn(1), and Zn(2), the other Zn(6), Zn(5), Zn(4) and Zn(3). The five-coordinate Zn(II) centres (Zn(2), Zn(3), Zn(6) and Zn(7)) are at the end of the respective zippers. The average Zn–Zn distance in the dinuclear complexes is 3.55 Å. Zn(1) and Zn(2) share a coordination environment

Table 2 Selected bond lengths (Å) and angles (°) for the main residue of the disordered complex $Li[Zn_2(HL1)]_4(PO_4)_2(PF_6)_3\cdot(CH_3OH)$

Molecule 1

Zn(1)–O(3)	2.137(11)	Zn(4)–O(7)	2.092(6)	Zn(7)–N(15)	2.246(13)
Zn(1)–N(1)	2.171(7)	Zn(4)–N(6)	2.107(8)	Zn(7)–O(41)	1.898(11)
Zn(1)–O(1)	2.312(6)	Zn(4)–O(54)	1.972(6)	Zn(7)–N(16)	2.167(14)
Zn(1)–N(2)	2.104(7)	Zn(4)–O(9)	2.085(13)	Zn(7)–O(16)	1.879(10)
Zn(1)–O(51)	1.959(5)	Zn(4)–N(5)	2.144(8)	Zn(7)–O(15)	2.139(10)
Zn(1)–O(13)	2.082(6)	Zn(4)–O(5)	2.659(18)	Zn(8)–O(42)	1.969(5)
Zn(2)–O(4)	2.051(7)	Zn(5)–O(5)	2.061(16)	Zn(8)–N(13)	2.181(8)
Zn(2)–N(4)	2.102(12)	Zn(5)–O(43)	2.030(7)	Zn(8)–O(15)	2.079(6)
Zn(2)–O(3)	1.954(7)	Zn(5)–O(11)	2.065(8)	Zn(8)–O(13)	2.514(6)
Zn(2)–O(52)	1.945(6)	Zn(5)–N(9)	2.225(15)	Zn(8)–N(14)	2.114(7)
Zn(2)–N(3)	2.128(15)	Zn(5)–N(10)	2.137(10)	Zn(8)–O(1)	2.070(6)
Zn(3)–N(8)	1.948(10)	Zn(5)–O(9)	2.318(13)	Zn(1)···Zn(2)	3.553(1)
Zn(3)–N(7)	2.201(15)	Zn(6)–O(11)	2.022(8)	Zn(3)···Zn(4)	3.529(1)
Zn(3)–O(7)	1.982(6)	Zn(6)–N(11)	2.196(14)	Zn(4)···Zn(5)	3.559(2)
Zn(3)–O(8)	2.213(14)	Zn(6)–O(12)	2.013(11)	Zn(5)···Zn(6)	3.561(2)
Zn(3)–O(53)	1.969(6)	Zn(6)–N(12)	2.089(9)	Zn(7)···Zn(8)	3.603(2)
O(41)–P(4)	1.541(8)	Zn(6)–O(44)	1.966(7)	Zn(1)···Zn(8)	3.479(1)
O(42)–P(4)	1.533(6)	O(43)–P(4)	1.542(7)	O(44)–P(4)	1.509(8)
O(51)–P(5)	1.532(6)	O(52)–P(5)	1.523(7)	O(53)–P(5)	1.526(6)
O(54)–P(5)	1.536(6)				
O(3)–Zn(1)–N(1)	89.8(3)	O(3)–Zn(1)–O(1)	162.6(2)		
O(3)–Zn(1)–N(2)	85.9(3)	O(3)–Zn(1)–O(51)	92.2(3)		
O(3)–Zn(1)–O(13)	116.5(2)	N(1)–Zn(1)–O(1)	72.9(2)		
N(1)–Zn(1)–N(2)	79.9(3)	N(1)–Zn(1)–O(51)	97.2(3)		
N(1)–Zn(1)–O(13)	151.2(2)	O(1)–Zn(1)–N(2)	91.0(2)		
O(1)–Zn(1)–O(51)	90.0(2)	O(1)–Zn(1)–O(13)	80.5(2)		
N(2)–Zn(1)–O(51)	176.6(3)	N(2)–Zn(1)–O(13)	89.9(3)		
O(51)–Zn(1)–O(13)	93.5(2)	O(3)–Zn(2)–N(3)	90.4(5)		
O(3)–Zn(2)–N(4)	137.0(4)	O(3)–Zn(2)–O(4)	112.9(8)		
O(3)–Zn(2)–O(52)	98.5(4)	N(3)–Zn(2)–N(4)	79.0(4)		
N(3)–Zn(2)–O(4)	86.3(5)	N(3)–Zn(2)–O(52)	170.1(3)		
N(4)–Zn(2)–O(4)	107.9(8)	N(4)–Zn(2)–O(52)	91.5(4)		
O(4)–Zn(2)–O(52)	94.2(2)	O(7)–Zn(3)–N(8)	139.0(4)		
O(7)–Zn(3)–N(7)	89.9(3)	O(7)–Zn(3)–O(8)	102.1(4)		
O(7)–Zn(3)–O(53)	100.5(2)	N(7)–Zn(3)–N(8)	81.3(4)		
N(7)–Zn(3)–O(8)	78.2(4)	N(7)–Zn(3)–O(53)	165.9(4)		
N(8)–Zn(3)–O(8)	114.9(5)	N(8)–Zn(3)–O(53)	96.6(4)		
O(8)–Zn(3)–O(53)	90.3(3)	O(7)–Zn(4)–N(5)	93.5(3)		
O(7)–Zn(4)–O(5)	160.3(4)	O(7)–Zn(4)–O(54)	95.3(4)		
O(7)–Zn(4)–N(6)	93.2(3)	N(5)–Zn(4)–O(5)	66.9(4)		
O(7)–Zn(4)–O(9)	126.4(4)	N(5)–Zn(4)–N(6)	80.4(3)		
N(5)–Zn(4)–O(54)	96.1(3)	N(5)–Zn(4)–O(9)	138.2(4)		
O(5)–Zn(4)–N(6)	86.3(4)	O(5)–Zn(4)–O(54)	84.7(4)		
O(5)–Zn(4)–O(9)	73.2(4)	N(6)–Zn(4)–O(54)	171.0(3)		
N(6)–Zn(4)–O(9)	85.1(4)	O(54)–Zn(4)–O(9)	92.1(4)		
O(11)–Zn(5)–N(9)	90.3(4)	O(11)–Zn(5)–O(9)	163.4(4)		
O(11)–Zn(5)–N(10)	84.8(3)	O(11)–Zn(5)–O(43)	97.8(3)		
O(11)–Zn(5)–O(5)	114.7(5)	N(9)–Zn(5)–O(9)	73.1(4)		
N(9)–Zn(5)–N(10)	79.2(4)	N(9)–Zn(5)–O(43)	92.1(3)		
N(9)–Zn(5)–O(5)	151.5(5)	O(9)–Zn(5)–N(10)	92.2(5)		
O(9)–Zn(5)–O(43)	82.8(4)	O(9)–Zn(5)–O(5)	81.5(5)		
N(10)–Zn(5)–O(43)	171.0(4)	N(10)–Zn(5)–O(5)	89.3(6)		
O(43)–Zn(5)–O(5)	97.3(3)	O(11)–Zn(6)–N(11)	89.6(4)		
O(11)–Zn(6)–O(12)	108.9(4)	O(11)–Zn(6)–N(12)	138.0(4)		
O(11)–Zn(6)–O(44)	92.1(3)	N(11)–Zn(6)–N(12)	77.3(4)		
N(11)–Zn(6)–O(12)	81.2(4)	N(11)–Zn(6)–O(44)	178.2(4)		
N(12)–Zn(6)–O(12)	108.2(4)	N(12)–Zn(6)–O(44)	101.0(4)		
O(12)–Zn(6)–O(44)	98.8(4)	O(15)–Zn(7)–N(15)	86.2(5)		
O(15)–Zn(7)–N(16)	115.8(5)	O(15)–Zn(7)–O(16)	109.7(5)		
O(15)–Zn(7)–O(41)	98.2(5)	N(15)–Zn(7)–N(16)	74.7(6)		
N(15)–Zn(7)–O(16)	83.3(4)	N(15)–Zn(7)–O(41)	171.4(5)		
N(16)–Zn(7)–O(16)	127.1(5)	N(16)–Zn(7)–O(41)	96.7(6)		
O(16)–Zn(7)–O(41)	102.1(4)	O(15)–Zn(8)–N(13)	92.9(3)		
O(15)–Zn(8)–O(13)	162.4(3)	O(15)–Zn(8)–N(14)	94.6(3)		
O(15)–Zn(8)–O(42)	95.1(2)	O(15)–Zn(8)–O(1)	121.5(2)		
N(13)–Zn(8)–O(13)	69.6(3)	N(13)–Zn(8)–N(14)	79.8(3)		
N(13)–Zn(8)–O(42)	97.6(3)	N(13)–Zn(8)–O(1)	144.1(3)		
O(13)–Zn(8)–N(14)	84.4(3)	O(13)–Zn(8)–O(42)	85.8(3)		
O(13)–Zn(8)–O(1)	76.1(3)	N(14)–Zn(8)–O(42)	170.1(3)		

Table 2 *(Contd.)*

Molecule 1			
N(14)–Zn(8)–O(1)	87.0(2)	O(42)–Zn(8)–O(1)	89.8(2)
Zn(1)–O(3)–Zn(2)	120.5(6)	Zn(4)–O(7)–Zn(3)	120.0(3)
Zn(5)–O(11)–Zn(6)	121.2(4)	Zn(8)–O(15)–Zn(7)	117.3(4)
Zn(1)–O(1)–Zn(8)	105.0(2)	Zn(4)–O(5)–Zn(5)	97.0(3)
Zn(5)–O(9)–Zn(4)	107.7(5)	Zn(8)–O(13)–Zn(1)	98.0(3)
O(44)–P(4)–O(42)	110.3(4)	O(44)–P(4)–O(41)	111.1(5)
O(42)–P(4)–O(41)	109.8(4)	O(44)–P(40–O(43)	114.6(4)
O(42)–P(4)–O(43)	102.9(4)	O(41)–P(4)–O(43)	107.7(4)
O(52)–P(5)–O(53)	110.0(4)	O(52)–P(5)–O(51)	114.4(4)
O(53)–P(5)–O(51)	108.6(4)	O(52)–P(5)–O(54)	110.5(4)
O(53)–P(5)–O(54)	109.5(4)	O(51)–P(5)–O(54)	103.6(3)
Hydrogen bonding			
O(2)···O(16)	2.574(10)	O(6)···O(12)	2.538(17)
O(10)···O(8)	2.57(2)	O(14)···O(4)	2.598(18)
O(2)···H–O(16)	165.4	O(6)···H–O(12)	163.1
O(10)···H–O(8)	168.6	O(14)···H–O(4)	177.1

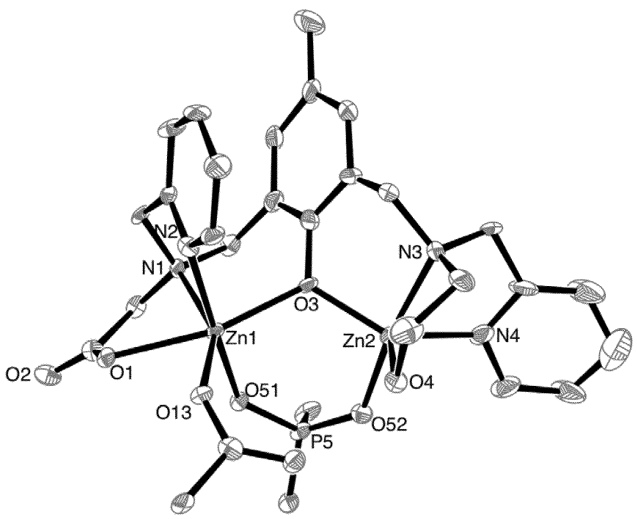

Fig. 4 ORTEP plot of a fragment of the complex cation of $Li[Zn_2(HL1)]_4(PO_4)_2(PF_6)_3\cdot(CH_3OH)$. Thermal probability ellipsoids are drawn at the 50% probability level. Hydrogen atoms are omitted for clarity.

of an $HL1^{2-}$ ligand with an unsymmetrical bridge through the μ-phenoxo oxygen donor O(3); likewise, Zn(3) and Zn(4), Zn(5) and Zn(6), and Zn(7) and Zn(8) each share an $HL1^{2-}$ ligand. The six-coordinate geometry of Zn(1) and Zn(8) (and by analogy Zn(4) and Zn(5)) is made up of bonds to the μ-phenoxide (Zn(1)–O(3)), the pyridine nitrogen (Zn(1)–N(2)), the tertiary nitrogen (Zn(1)–N(1)), the PO_4^{3-} oxygen (Zn(1)–O(51)), the oxygen of an adjacent carboxylate (Zn(1)–O(13)) and the oxygen of the carboxylate from the $HL1^{2-}$ shared with Zn(8) (Zn(1)–O(1)). Thus, Zn(1) and Zn(8) (and similarly Zn(4) and Zn(5)) are bridged through a bifurcation of the oxygen donors of the acetic acid arms of the $HL1^{2-}$ ligand, one oxygen from each ligand. In each case, two of the interactions are relatively long (Zn(1)–O(1), Zn(8)–O(13), Zn(4)–O(5), Zn(5)–O(9)) whereas the others are significantly shorter (Zn(1)–O(13), Zn(8)–O(1), Zn(4)–O(9), Zn(5)–O(5)). The Zn(4) and Zn(8) sites, which have the long (>2.5 Å) Zn–O(carboxylate) bonds, are noticeably more distorted from the octahedral geometry, and in fact may be better described as edge-bridged trigonal-bipyramidal structures. The bifurcated nature of this interaction is reminiscent of that seen for Asp_{50} in the structure of GpdQ.[13]

The five-coordinate Zn(2) (and by analogy Zn(3), Zn(6) and Zn(7)) ions are trigonal-bipyramidal, where the amine nitrogen and phosphate oxygen atoms are *trans*. The five-coordinate geometry is comprised of bonds to the bridging phenoxide (Zn(2)–O(3)), a pyridine nitrogen (Zn(2)–N(4), a tertiary nitrogen (Zn(2)–N(3)), a hydroxyl oxygen (Zn(2)–O(4)) and a phosphate oxygen (Zn(2)–O(52)). Strong hydrogen bonds link the hydroxyl oxygen of one Zn_2HL1 unit to the uncoordinated carboxylate oxygen of a neighbouring Zn_2HL1 unit (for example: O(4)–H···O(14) 2.597(4) Å, O(4)–H···O(14) 177 °).

Mass spectrometry

The ligand precursor H_2EtL1 displays the expected low-resolution positive-ion mass spectrum with *m/z* 479.21. The ESI-MS of the zinc complex with the $HL1^{2-}$ ligand, characterised as $[Zn_2(HL1)(CH_3COO)](PF_6)$ in acetonitrile indicates the presence of $[Zn_2(HL1)(CHOO)]^+$ (*m/z* 625.06, 623.06 and 621.06), $[Zn_2(HL1)]^+$ (*m/z* 579.06, 577.06 and 575.06) with the most prominent peaks typical of the isotopic pattern expected for a di-Zn(II) complex. In addition, the species $[Zn(HL1)]^+$ (*m/z* 517.14, 515.14 and 513.14) was also present. The ESI-MS in water–acetonitrile (90 : 10) indicates the presence of $[Zn(HL1) + H]^+$ (*m/z* 513.14) with an isotope pattern consistent with the presence of only one metal ion. In the presence of two equivalents of zinc acetate, in the same solvent mixture, peaks attributed to $[Zn(HL1)(CH_3COO)(H_2O)_6 + 2H]^+$ (*m/z* 681.23, 682.23 and 683.23) and $[Zn_2(HL1)(CH_3COO)(H_2O)_6]^+$ (*m/z* 743.14, 745.14, 747.14 and 748.14) were present, the latter with an isotope pattern indicative of a di-Zn(II) complex (see ESI†). In order to probe the hydrolysis reaction of $[Zn_2(HL1)(\mu\text{-}CH_3COO)](PF_6)$, the complex was reacted with the substrate bNPP for 24 h at 50 °C in a water–acetonitrile (90 : 10) solution and the mass spectrum recorded. The most prominent peak was at *m/z* 513.14, assigned to $[Zn(HL1) + H]^+$; no peaks assigned to phosphate-containing species were observed. The addition of excess Zn(II) (as Zn(II)

acetate) resulted in the appearance of more prominent di-Zn(II) species (*m*/*z* 745.14 and 747.14).

Potentiometric studies

The pK_a values of H_3L1 were determined from the potentiometric titration curve obtained when the ligand was titrated in an acetonitrile–water solution (1 : 4, v/v) at 25 °C, $I = 0.1$ (Et_4NClO_4) with Et_4NOH. The pK_a values at low (<3) and high (>9) pH were determined iteratively after fitting the mid-pH range and then holding the obtained fitted parameters fixed in order to fit the extremes of the curve. Once a satisfactory fit was obtained, all the pK_a values were allowed to refine freely in order to minimise the complete set. The pK_a values determined were 2.95, assigned to the carboxylic acid, 4.97 and 7.53, assigned to the two pyridine nitrogen atoms,[45] and 10.97, which corresponds to the deprotonation of the alcoholic oxygen.

Potentiometric titrations of Zn(II) and H_3L1 with base in the pH range 2.0–8.5 in an acetonitrile–water solution (1 : 4, v/v) yielded $\log K_1 = 5.98$ and $\log K_2 = 3.35$ as the simplest model. The fit to the two binding constants was reproducible over a number of different titrations and, when more complicated models including hydroxo ligands were added these were routinely rejected as valid models unless the most rigorous fitting conditions were applied. The simplest model was therefore accepted. The relative magnitudes of the binding constants suggest that one Zn(II) is bound relatively tightly to $HL1^{2-}$, and the second more loosely.

Phosphodiesterase-like activity

The phosphatase-like activity of the proposed $[Zn_2(HL1)(CH_3COO)](PF_6)\cdot H_2O$ was measured under conditions of excess substrate, using bNPP (bis-nitrophenyl phosphate). The species tested was the initially prepared Zn_2 complex and not the supramolecular Zn_8 complex, which resulted during growth of diffraction-quality crystals. Under the conditions of the mass spectrometer for the complex formulated as $[Zn_2(HL1)(CH_3COO)](PF_6)\cdot H_2O$, the acetate is retained in the absence of substrate, however exposure to bNPP results in a species in which the acetate is lost, albeit on prolonged standing. A number of assumptions can be made concerning the catalytically active species. It could be assumed that, to produce a catalytically active species, the acetate ligand partially or completely dissociates, resulting in a complex with either terminal or bridging aqua ligands, $[Zn_2(HL1)(OH_2/OH)_x]^{m+}$.[28–31,33–35] Alternatively, the active species may be an aqua complex $[Zn_2(HL1)(\mu\text{-}CH_3COO)(OH_2)_x]^+$ in which the μ-acetato ligand is retained.

The hydrolysis of bNPP was examined in the presence of added zinc ions and as a function of the concentration of $[Zn_2(HL1)(\mu\text{-}CH_3COO)]^+$. In all experiments, the effect of added Zn(II) was negligible up until the addition of two equivalents when a slight rate enhancement was observed. This observation suggests that the most significant active species in solution is a di-Zn(II) complex based on $[Zn_2(HL1)(\mu\text{-}CH_3COO)_n(OH_2/OH)_x]^{m+}$ ($n = 0$ or 1). It is possible that the presence of substrate stabilises or aids in the assembly of the di-Zn(II) site, analogous to the suggestion made that in some phosphoesterase systems the reconstitution of a catalytically competent enzyme may only occur in the presence of substrates.[2,46]

The effect of complex concentration, based on $[Zn_2(HL1)(\mu\text{-}CH_3COO)](PF_6)\cdot H_2O$ (pH 9.0; 50 °C), on the rate of hydrolysis of bNPP (1 mM) was linear for concentrations of complex from 0.05–0.25 mM (Fig. 5), with a second order rate constant of $7.55 \pm 0.26 \times 10^{-3}$ M^{-1} s^{-1}. The addition of extra Zn(II) had no effect on the rates of the reactions. The pH dependence on the rate of bNPP cleavage by the complex displays a sigmoidal behaviour in the pH range 7–9.5. The data were fitted using an equation derived for a monoprotic system,[47] yielding a pK_a value of 7.87 (Fig. 6) for the catalytically relevant agent in the model substrate complex.

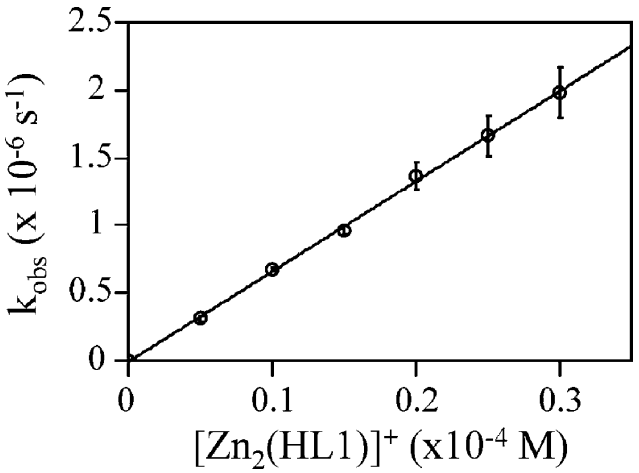

Fig. 5 Dependence of the pseudo-first order rate constant on the concentration of $[Zn_2(HL1)]^+$ in 88 mM CHES buffer at pH 9.0, 50 °C, containing 88 mM $LiClO_4$.

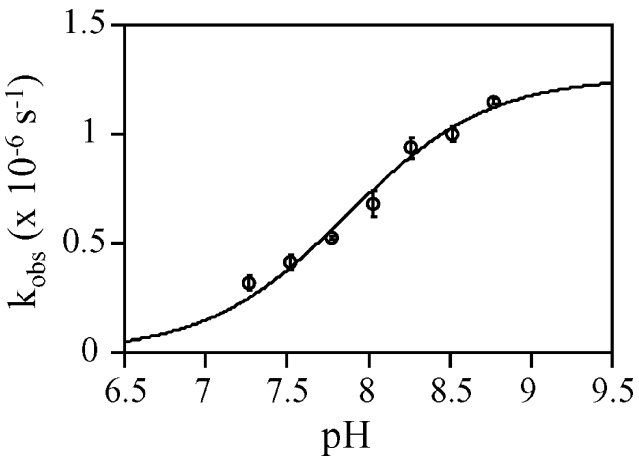

Fig. 6 pH dependence on the reaction rate for $[Zn_2(HL1)]^+$.

The initial rate of bNPP cleavage has also been determined as a function of substrate concentration, revealing typical saturation behaviour (Fig. 7). The data were fitted by non-linear regression, using the Michaelis–Menten equation,

$$Rate = \frac{V_{max}[S]}{[S] + K_M},$$

where $V_{max} = k_{cat}[Zn_2(complex)]$

The substrate concentration at half-maximal rate (K_M) is $1.96 \pm 0.25 \times 10^{-3}$ M with $V_{max} = 4.37 \pm 0.51 \times 10^{-11}$ mol L s^{-1} and

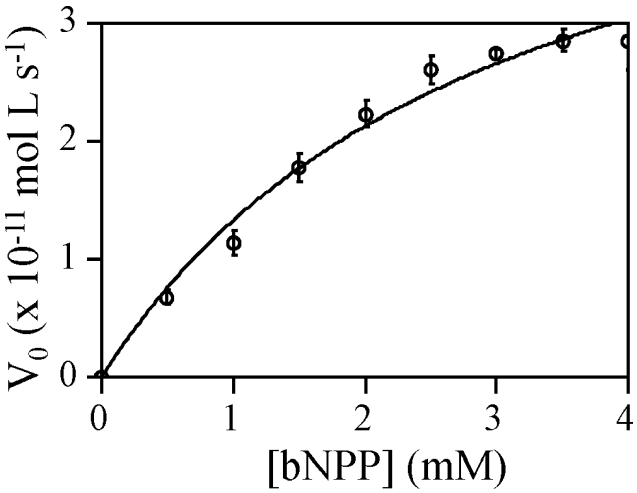

Fig. 7 Dependence on the rate of bNPP cleavage by $[Zn_2(HL1)]^+$ (0.02 mM) at pH 9.0, 50 °C, 88 mM $LiClO_4$, [CHES buffer] 88 mM.

the corresponding $k_{cat} = 1.26 \pm 0.06 \times 10^{-6}$ s^{-1}. The indicative substrate binding constant ($K_b = 1/K_M$) is 510 M^{-1}, suggesting that bNPP is a stronger ligand for $[Zn_2(HL1)]^{2+}$ than it is for the H_2L2^- complex ($K_b = 16.3$ M^{-1}).[28] For the analogue $[Zn_2(HL2)(\mu\text{-}CH_3COO)(H_2O)](PF_6)$[28] (2,6-bis([(2-pyridylmethyl)(2-hydroxyethyl)amino]methyl)-4-methylphenol (H_2L2^-)) under similar reaction conditions $K_M = 6.15 \times 10^{-2}$ M and $k_{cat} = 4.60 \times 10^{-6}$ s^{-1} have been reported.[28]

Mechanistic implications

$[Zn_2(HL1)(CH_3COO)](PF_6)$ and $[Zn_2(HL2)(\mu\text{-}CH_3COO)(H_2O)](PF_6)\cdot H_2O$ display catalytically relevant pK_a values of 7.87 and 7.13, respectively.[28] Theoretical studies have indicated that the Zn(II)–alcohol has a lower pK_a than the Zn(II)–water in the same molecule.[48] This, combined with studies in non-aqueous solvents, led to the suggestion that for $[Zn_2(HL2)(\mu\text{-}CH_3COO)(H_2O)](PF_6)$, the alcohol hydroxyl, with a pK_a of 7.20, is the nucleophile.[28] The identity of the nucleophile is less clear for $[Zn_2(HL1)(\mu\text{-}CH_3COO)](PF_6)\cdot H_2O$. From the pH dependence studies, the active species was determined to display a pK_a of 7.87, typical of that for the deprotonation of a terminal aqua ligand,[49] although the pK_a for the deprotonation of a bridging hydroxide is also within this range.[50–52] The assignment of the catalytic pK_a is further complicated by the observation that the magnitude of the Zn(II)–aqua pK_a depends on, amongst other factors, the stereochemistry around the Zn(II) ion, the metal–metal ion separation, and the extent of hydrogen bonding. Thus, pK_a values as low as ~4.44 and as high as 9 are observed with apparently little discrimination between the pK_a exhibited by the monomeric and dimeric Zn(II) complexes.[28,48,49,52–62]

The assignment of the catalytically relevant pK_a of the Zn(II) complex of $HL1^{2-}$ to either a terminal or metal ion bridging hydroxide is in agreement with the corresponding assignments in OPH, OpdA, GpdQ and various other binuclear metallohydrolases.[2,17,19,31,63] A combination of the experimental and theoretical (computational) studies of OPH suggests that the bridging hydroxide with a pK_a of 8.4 is the nucleophile in phosphate ester hydrolysis.[20,63,64] Other binuclear metallohydrolases that are reported to initiate hydrolysis with the μ-hydroxide include, amongst others, some purple acid phosphatases, arginases and ureases.[31,65–69] In contrast, a recent crystallographic study showing trapped substrates bound to the active site of OpdA suggests that in this enzyme the nucleophile is monodentately bound to the α-metal site (Fig. 1).[20] Clearly, there is substantial ambiguity and variety with respect to assigning nucleophiles. In an attempt to reconcile these different strategies, it has been suggested that the μ-hydroxo is the actual source of the nucleophile, but that substrate binding triggers the displacement of the μ-OH to form a quasi-terminal hydroxide, coordinated predominantly to the more buried or α- site.[70,71]

While it is no trivial task to deconvolute the precise details of the catalytic mechanism(s) employed by binuclear hydrolytic systems, it has emerged that subtle variations in the first and second coordination environment and differences in the metal ion composition have less subtle effects on that mechanism(s).[2] For instance, for purple acid phosphatase extracted from the pig uterine fluid (uteroferrin) the likely nucleophile for the FeFe and FeZn metal ion combinations is a terminally bound hydroxide,[72] while for the GaZn, FeNi and possibly FeMn combinations, the μ-hydroxide is the likely candidate nucleophile.[31,35] Similarly, different nucleophiles are proposed by different groups for the highly homologous OPH and OpdA (~90% sequence identity).[9,10,17]

In summary, despite the ambiguity of the assignment of the catalytically relevant pK_a values for the Zn(II) complex of $HL1^{2-}$, the mechanistic features of the model system are in good agreement with those of the corresponding enzymatic systems.

Conclusions

Effective biomimetics are expected to display both the structural and functional characteristics of the metallobiosite.[24–29] In the case of both $HL1^{2-}$ and H_2L2^- [28], the zinc complexes mimic aspects of the features of the metallobiosites of OPH, OpdA and GpdQ, $HL1^{2-}$, in particular, appearing to present a strong and loose binding site, analogous to the situation observed in the enzymes. Modelling the activity and the exact nucleophilic agent is more problematic. The catalytic activity of the Zn(II) complexes of $HL1^{2-}$ and $HL2^-$ appears typical of that exhibited by similar complexes, although it is difficult to make definitive comparisons due to the different reaction conditions employed.[28,52] Whilst the k_{cat} of ~1.5×10^{-6} s^{-1} represents considerable enhancement over the uncatalyzed rate (1.1×10^{-11} s^{-1})[73] the enhancement does not approach the catalytic rate of the metalloenzymes (the catalytic rates for OPH and OpdA are > 1000 s^{-1}).[13,15,16] There are strategies, however, that reportedly lead to an enhanced activity for biomimetic systems.[59,74] Considering the potential applications of OPH, OpdA and GpdQ for bioremediation, it is an attractive endeavour to develop more robust biomimetic systems exhibiting sufficient structural and functional stability to be used practically.

Experimental

Instrumental methods

NMR spectra were measured using Bruker AV400 (400 MHz) and AV500 (500 MHz) instruments. The spectra were recorded in $CDCl_3$, with chemical shifts reported in parts per million (ppm) and calibrated using the resonances for $CDCl_3$,

$\delta_H(CHCl_3)$ = 7.24 ppm and $\delta_C(CDCl_3)$ = 77.0 ppm. Low and high-resolution positive-ion mass spectra were obtained using either a Q-Star time-of-flight mass spectrometer, in methanol or acetonitrile, using 10% acetic or formic acid carrier liquid or a Finnigan MAT 900 XL mass spectrometer and methanol solutions for the ligand, and acetonitrile for the metal complex. All samples were subjected to electrospray ionisation, with voltages tuned to optimise the signals. The predicted isotopic splitting patterns of peaks were calculated using the program Molecular Weight Calculator.[75] Infrared spectroscopy was performed with a Perkin Elmer FT-IR SPECTRUM 2000 spectrometer with a Smiths DuraSamplIR II ATR diamond window. Elemental analyses were performed using the microanalysis facilities at The University of Queensland.

Syntheses of the ligands and metal complex

2,6-Bis(chloromethyl)-4-methyl-phenol, *N*-(2-pyridylmethyl) glycine ethyl ester, *N*-(2-pyridylmethyl)-2-aminoethanol were prepared as described previously.[36–38]

[Ethyl-2-((2-hydroxy-3-(((2-hydroxyethyl)(pyridin-2-ylmethyl)-amino)methyl)-5-methylbenzyl)(pyridin-2-ylmethyl)amino)acetate] (H_2EtL1). H_2EtL1 was synthesised from 2,6-bis(chloromethyl)-4-methyl-phenol, *N*-(2-pyridylmethyl)glycine ethyl ester and *N*-(2-pyridylmethyl)-2-aminoethanol using a statistical reaction. Thus, *N*-(2-pyridylmethyl) glycine ethyl ester (1.12 g, 5.76 mmol) and *N*-(2-pyridylmethyl)-2-aminoethanol (0.88 g, 5.8 mmol) were dissolved in 9 mL of tetrahydrofuran (THF) with 1.15 g triethylamine (TEA) (11.48 mmol). Separately, 2,6-bis-(chloromethyl)-4-methyl-phenol (1.18 g, 5.76 mmol) was dissolved in 8 mL dichloromethane (DCM) and added dropwise under stirring into the TEA solution at 0 °C. The mixture was stirred at room temperature for 48 h, the precipitated TEA·HCl was filtered off, and the solvent was removed by rotary evaporation. The residue was taken up in DCM (50 mL), washed with concentrated aqueous NaCl (20 mL), the organic layer dried over anhydrous sodium sulfate, filtered and the solvent removed *in vacuo*, to yield an orange oil (2.35 g). NMR and TLC of the mixture revealed a combination of three products. The separation of the products was achieved with column chromatography (silica; 80 : 20, ethyl acetate–methanol). The first product eluted from the column (R_f: 0.89) was determined to be [diethyl-2,20-(2-hydroxy-5-methyl-1,3-phenylene)bis(methylene)bis((pyridin-2-ylmethyl)azanediyl)diacetate] (0.4 g). NMR δ_H/ppm (500 MHz, $CDCl_3$): 1.21 (6H, t, J = 7.15 Hz, CH_2CH_3), 2.18 (3H, s, Ar–CH_3), 3.37 (4H, s, CH_2), 3.84 (4H, s, CH_2), 3.93 (4H, s, CH_2), 4.12 (2H, q, J = 7.22 Hz, CH_2CH_3), 6.91 (2H, s, Ar–H), 7.09 (2H, qd, J = 1.65 Hz, 1.17, py–CH), 7.45 (2H, dt, J = 7.89 Hz, 1.01, py–CH) 7.59 (2H, td, J = 3.85 Hz, 1.80, py–CH) 8.47 (2 H, dq, J = 4.93 Hz, 0.91, py–CH). NMR δ_C/ppm (500 MHz, $CDCl_3$): 14.12 (CH_2CH_3), 20.39 (Ar–CH_3), 54.32, 59.41, 60.43 (CH_2), 122.02 (Ar–C), 123.10, 123.14 (py–CH), 127.56 (Ar–CH), 130.05 (Ar–C), 136.56, 148.77 (py–CH), 153.48 (Ar–C), 158.74 (py–C), 171.31 (C=O). m/z: 521.22 ($C_{29}H_{37}N_4O_5$, M^+), 479.22 ($C_{27}H_{35}N_4O_4$), 327.17 ($C_{19}H_{23}N_2O_3$), 286.16 ($C_{17}H_{22}N_2O_2$), 195.13 ($C_{10}H_{15}N_2O_2$). The second product to be eluted (R_f: 0.59) was identified as the target product (0.65 g). NMR δ_H/ppm (500 MHz, $CDCl_3$): 1.19 (3H, t, J = 7.15 Hz, CH_2CH_3), 2.15 (3H, s, Ar–CH_3), 2.70 (2H, t, J = 5.18 Hz, NCH_2CH_2), 3.33 (2H, s, CH_2), 3.66 (2H, t, J = 5.28 Hz, CH_2OH), 3.72 (2H, s, CH_2), 3.79 (2H, s, CH_2), 3.80 (2H, s, CH_2), 3.92 (2H, s, CH_2), 4.12 (2H, q, J = 7.14 Hz, CH_2CH_3), 6.78 (1H, d, J = 1.90 Hz, Ar–H), 6.85 (1H, d, J = 1.85 Hz, Ar–H), 7.03 (1H, qd, J = 1.67 Hz, 1.05, py–CH), 7.11 (1H, qd, J = 1.63 Hz, 1.03, py–CH), 7.34 (1H, dt, J = 7.88 Hz, 1.01, py–CH), 7.44 (1H, td, J = 3.88 Hz, 1.85, py–CH), 7.59 (1H, td, J = 3.84 Hz, 1.82, py–CH), 8.40 (1H, dq, J = 4.93 Hz, 0.86, py–CH), 8.50 (1H, dq, J = 4.75 Hz, 0.83, py–CH). NMR δ_C/ppm (500 MHz, $CDCl_3$): 14.08 (CH_2CH_3), 20.29 (Ar–CH_3), 53.96, 54.50, 55.05, 55.70, 58.87, 59.09, 59.41, 60.52 (CH_2), 121.84, 121.99 (py–CH), 122.19, 122.36 (Ar–C), 122.99, 123.08 (py–CH), 127.45 (Ar–C), 129.88, 130.70 (Ar–CH), 136.38, 136.70, 148.46, 148.80 (py–CH), 153.51 (Ar–C), 157.96 (py–C), 171.03 (C=O). m/z: 479.22 ($C_{27}H_{35}N_4O_4$, M^+), 388.22 ($C_{21}H_{30}N_3O_4$), 327.17 ($C_{19}H_{23}N_2O_3$), 285.17 ($C_{17}H_{21}N_2O_2$), 242.29 ($C_{15}H_{18}N_2O$). The third product eluted (R_f: 0.30) was symmetric H_3L2 (0.33 g). NMR δ_H/ppm (500 MHz, $CDCl_3$): 2.17 (3H, s, Ar–CH_3); 2.69 (4H, t, J = 5.20 Hz, 2 × NCH_2CH_2OH); 3.64 (4H, t, J = 5.23 Hz, 2 × NCH_2CH_2OH); 3.72 (4H, s, 2 × CH_2); 3.84 (4H, s, 2 × CH_2); 6.79 (2H, s, 2 × Ar–H); 7.10 (2H, qd, J = 1.70 Hz, 1.10, py–CH), 7.26 (2H, dt, J = 7.88 Hz, 1.19, py–CH), 7.54 (2H, td, J = 3.85 Hz, 1.85, py–CH), 8.49 (2H, dq, J = 5.13 Hz, 0.85, py–CH). NMR δ_C/ppm (500 MHz, $CDCl_3$): 20.38 (Ar–CH_3), 55.75, 55.99, 59.31 59.34 (CH_2), 122.14, 123.16 (py–CH), 123.70, 127.56, 130.32 (Ar–CH), 136.68, 148.81 (py–CH), 153.71 (Ar–CH), 158.79 (py–CH). m/z: 437.21 ($C_{25}H_{33}N_4O_3$, M^+), 285.17 ($C_{17}H_{21}N_2O_2$), 242.29 ($C_{15}H_{18}N_2O$), 153.11 ($C_8H_{13}N_2O$).

Lithium salt of [2-((2-hydroxy-3-(((2-hydroxyethyl)(pyridin-2-ylmethyl)amino)methyl)-5-methylbenzyl)(pyridin-2-ylmethyl)amino)-acetic acid] (LiH_2L1). A methanol solution of LiOH (0.1 M) was prepared from 0.2115 g LiOH in 100 mL methanol. H_2EtL1 (0.1087 g, 0.227 mmol) was dissolved in MeOH (1 mL), 2.27 mL of the LiOH–methanol solution was added and the mixture stirred for 48 h. Removal of the solvent *in vacuo* giving LiH_2L1 as a yellow oil (0.10 g). NMR δ_H/ppm (400 MHz, $CDCl_3$): 2.54 (2, NCH_2CH_2), 3.30–3.85 (12, CH_2), 4.12, 6.61–6.71 (2, Ar–H), 6.99–8.33 (8, py–CH). NMR δ_C/ppm (400 MHz, $CDCl_3$): 19.69 and 19.87 (Ar–CH_3), 51.00–59.27 (CH_2), 60.61 (CH_2), 121.64 (py–CH), 121.88 (py–CH), 122.02 (Ar–*tert*-C), 122.69 (py–CH), 122.80 (py–CH), 136.39 (Ar–CH), 136.43 (py–CH), 136.69 (py–CH), 148.33 (py–CH), 157.51 (Ar–C), 158.30 (py–C), 159.61 (py–C), 171.20 (C=O).

$[Zn_2(HL1)(CH_3COO)](PF_6)\cdot H_2O$ and $Li[Zn_2(HL1)]_4(PO_4)_2(PF_6)_3\cdot(CH_3OH)$. LiH_2L1 (0.10 g, 0.219 mmol) was dissolved in methanol (1 mL). To this was added zinc acetate (0.0481 g, 0.219 mmol) dissolved in methanol dropwise with stirring. The resulting mixture was refluxed gently for 30 min then permitted to cool to room temperature. $NaPF_6$ (0.0550 g, 0.327 mmol) was dissolved in methanol (4 mL) and added and the solution was left to sit at room temperature. Slow evaporation and subsequent filtration produced a creamy white solid (53.6 mg, 77%). Found: C 40.75, H 4.11, N 7.00%. Calcd for $[Zn_2(C_{25}H_{28}N_4O_4)(CH_3COO)](PF_6)\cdot H_2O$: C 40.47, H 4.15, N 7.00%. NMR δ_H/ppm (400 MHz, DMSO): 1.98 (Ar–CH_3), 2.06 (NCH_2CH_2OH), 2.78 (CH_2OH), 2.16–3.23 (CH_2), 3.51–4.04 (CH_2), 6.54 and 6.66 (ArH), 6.80–8.55 (py–CH). NMR δ_C/ppm (400 MHz, DMSO): 19.70 and 19.77 (CH_3), 54.65, 55.33, 55.95, 56.72, 58.25, 58.85, 60.95 (CH_2), 121.76 (Ar–C),

123.05, 123.31, 123.81, 124.61 (py–CH), 131.79 (Ar–CH), 139.02, 139.74, 146.55, 147.26 (py–CH), 154.96 (Ar–C), 159.65 (py–C), 173.05 (C=O), 177.75 (Ar–C). ES-MS *m/z*: 623.10 and 625.1 $[Zn_2C_{25}H_{28}N_4O_4(CHOO)]^+$; 577.09 and 579.1 $[Zn_2C_{25}H_{27}N_4O_4]^+$; 513.17 $[ZnC_{25}H_{29}N_4O_4]^+$. FT-IR spectra (υ/cm^{-1}): 1605.23 (m, C=O str), 1568.99 (m, phenol and py C=C str), 1478.21 (m, py CH str), 1433.29 (m, py CH stretch), 1397.61 (m, CH_2CO def), 1267.72 (w, tertiary NC str), 1057.55, 1019.42 (w, COH str) 824.80 (*vs.* PF_6^-), 797.90, 765.92 (m, m, py CH def), 554.96 (s, PF_6^-).

Crystallisation of the complex proved to be difficult. A screening method was devised using crystallisation wells to screen solution environments for precipitating crystals. Acetate, nitrate, sulfate and phosphate anions were screened with differing quantities of the counter ion PF_6^- or ClO_4^-. The only environment to produce crystals was in the presence of hexafluorophosphate. Thus, the bulk reaction mixture was left to stand in the presence of PF_6^- resulting, after 4 d, a small crystal suitable for X-ray diffraction studies. This complex was subsequently characterised crystallographically as $Li[Zn_2(HL1)]_4(PO_4)_2(PF_6)_3{\cdot}(CH_3OH)$.

Crystallographic measurements

X-Ray diffraction data for a crystal of $Li[Zn_2(HL1)]_4(PO_4)_2(PF_6)_3{\cdot}(CH_3OH)$ were collected with a Bruker APEX II diffractometer with graphite monochromated MoKα ($\lambda = 0.71073$ Å) radiation. The structure was solved by direct methods using SIR97[76] and refined on F^2 using SHELXL-97[77] running within the WinGX interface.[78] Plots were drawn using the ORTEP program.[79] The hydrogen positions for the alcohol, methylene and coordinated water molecules were calculated and included in the final refinement cycle. All non-hydrogen atoms were refined with anisotropic thermal parameters. Selected crystal data and details of refinements are given in Table 1.

Catalytic studies

Catalytic studies on the zinc complexes of H_3L1 were performed with bNPP, which hydrolyses to form 4-nitrophenolate and 4-nitrophenyl phosphate. The hydrolysis was followed by monitoring the formation of 4-nitrophenol at 50 °C at 400 nm. The extinction coefficient at 400 nm for 4-nitrophenol is pH dependent and was experimentally determined for each relevant pH to kinetic experiments. All studies were performed in 3 mL reaction aliquots using the substrate bNPP (30 mM stock), buffers (MES, HEPES, Tris, CHES, 100 mM, aq.), and catalytic species Zn_2H_2L1 and $Zn(NO_3)_2$ in acetonitrile (all at 1 mM). All experiments were run in triplicate. The protocol for initialising the hydrolysis reaction was to add 0.3 mL of an acetonitrile solution of the zinc complex to the calculated amount of buffer in the test tubes. Where appropriate, excess $Zn(NO_3)_2$ was added to the test tubes. 0.1 mL bNPP was added, the solution was mixed and the absorbance at 400 nm measured. The reaction vessels were placed in a 50 °C water bath and the absorbance recorded at specified time intervals. The zinc dependence of bNPP hydrolysis by the Zn_2H_2L1 was investigated by performing kinetic experiments at varying molar equivalents of $Zn(NO_3)_2$ added to the reaction mixture. Control experiments were also run in identical environments in the presence of $Zn(NO_3)_2$ and absence of complex. The final concentrations in 3 mL were as described above and the final concentrations of added zinc were 0, 0.1, 0.2, 0.3, 0.4, 0.6, 0.8 and 1 mM, respectively, leading to a 1–10-fold excess of zinc. The effect of pH on the hydrolytic reaction was studied in the pH range 6.5–10 with the Zn_2H_2L1, and no excess zinc. The reactions were followed to 5% of bNPP hydrolysis. The kinetic experiments, as a function of substrate concentration, were performed at pH 9. The concentration of bNPP in the final 3 mL reactions was 0.5, 1.0, 1.5 and 2.0 mM, respectively.

Potentiometric titrations

Titrant solutions of acid ($HClO_4$) were standardised against Borax and titrant solutions of Et_4NOH were standardised against the previously standardised $HClO_4$. Potentiometric titrations were performed with a Metrohm 665 Dosimat. The e.m.f. was measured with an ORION model 720A pH meter with a glass electrode. All titrations were carried out at a constant ionic strength of 0.1 M Et_4NClO_4 and were performed under a nitrogen atmosphere at 25 °C. For each titration the pH meter was calibrated using pH 6.88 and 4.00 buffers and a calibration titration was performed to determine E_o and pK_w values. Potentiometric titrations were performed on both the free ligands and in the presence of zinc perchlorate under a MeCN–H_2O saturated nitrogen atmosphere at 25 °C. The reaction vessel contained 2 mL of product (5 mM) in acetonitrile, acidified with 8 mL $HClO_4$ (6.8 mM). The final concentration of the product was therefore 1 mM in an acetonitrile–water (1 : 4, v/v) solution. The ionic strength was kept constant at 0.1 M with Et_4NClO_4. Calibration titrations were conducted using constant volume increments (0.02 mL) of 0.109 M Et_4NOH solution. Reactant titrations were performed by keeping the mV change constant (–4 mV). The curve fitting of all the data was performed using SUPERQUAD[80] and all pK_a values were reproducible within 0.5 units.

Acknowledgements

This work was funded by a grant from the Australian Research Council (DP0664039).

References

1 F. Ely, J. L. Foo, C. J. Jackson, L. R. Gahan, D. L. Ollis and G. Schenk, *Curr. Top. Biochem. Res.*, 2007, **9**, 63–78.
2 N. Mitic, S. J. Smith, A. Neves, L. W. Guddat, L. R. Gahan and G. Schenk, *Chem. Rev.*, 2006, **106**, 3338–3363.
3 E. Kimura, *Curr. Opin. Chem. Biol.*, 2000, **4**, 207–213.
4 E. Ghanem, Y. Li, C. Xu and F. M. Raushel, *Biochemistry*, 2007, **46**, 9032–9040.
5 M. M. Benning, J. M. Kuo, F. M. Raushel and H. M. Holden, *Biochemistry*, 1994, **33**, 15001–15007.
6 E. Ghanem and F. M. Raushel, *Toxicol. Appl. Pharmacol.*, 2005, **207**, S459–470.
7 D. P. Dumas, S. R. Caldwell, J. R. Wild and F. M. Raushel, *J. Biol. Chem.*, 1989, **264**, 19659–19665.
8 S. S. Rowland, M. K. Speedie and B. M. Pogell, *Appl. Environ. Microbiol.*, 1991, **57**, 440–444.
9 H. Yang, P. D. Carr, S. Y. McLoughlin, J.-W. Liu, I. Horne, X. Qiu, C. M. J. Jeffries, R. J. Russell, J. G. Oakeshott and D. L. Ollis, *Protein Eng.*, 2003, **16**, 135–145.
10 I. Horne, T. D. Sutherland, R. L. Harcourt, R. J. Russell and J. G. Oakeshott, *Appl. Environ. Microbiol.*, 2002, **68**, 3371–3376.
11 J. A. Gerlt and W. H. Y. Wan, *Biochemistry*, 1979, **18**, 4630–4638.
12 S. Y. McLoughlin, C. J. Jackson, J.-W. Liu and D. L. Ollis, *Appl. Environ. Microbiol.*, 2004, **70**, 404–412.
13 C. J. Jackson, P. D. Carr, J.-W. Liu and S. J. Watt, *J. Mol. Biol.*, 2007, **367**, 1047–1062.

14 C. J. Jackson, P. D. Carr, H.-K. Kim, J.-W. Liu, P. Herrald, N. Mitic, G. Schenk, C. A. Smith and D. L. Ollis, *Biochem. J.*, 2006.
15 G. A. Omburo, J. M. Kuo, L. S. Mullins and F. M. Raushel, *J. Biol. Chem.*, 1992, **267**, 13278–13283.
16 M. M. Benning, H. Shim, F. M. Raushel and H. M. Holden, *Biochemistry*, 2001, **40**, 2712–2722.
17 S. D. Aubert, Y. Li and F. M. Raushel, *Biochemistry*, 2004, **43**, 5707–5715.
18 M. M. Benning, J. M. Kuo, F. M. Raushel and H. M. Holden, *Biochemistry*, 1995, **34**, 7973–7978.
19 C. J. Jackson, H.-K. Kim, P. D. Carr, J.-W. Liu and D. L. Ollis, *Biochim. Biophys. Acta*, 2005, **1752**, 56–64.
20 C. J. Jackson, J.-L. Foo, H.-K. Kim, P. D. Carr, J.-W. Liu, G. Salem and D. L. Ollis, *J. Mol. Biol.*, 2008, **375**, 1189–1196.
21 V. E. Lewis, W. J. Donarski, J. R. Wild and F. M. Raushel, *Biochemistry*, 1988, **27**, 1591–1597.
22 H. Shim and F. M. Raushel, *Biochemistry*, 2000, **39**, 7357–7364.
23 M. Jarenmark, H. Carlsson and E. Nordlander, *C. R. Chim.*, 2007, **10**, 433–462.
24 R. Kramer and T. Gajda, *Perspect. Bioinorg. Chem.*, 1999, **4**, 209–240.
25 H. Carlsson, M. Haukka and E. Nordlander, *Inorg. Chem.*, 2004, **43**, 5681–5687.
26 M. Jarenmark, S. Kappen, M. Haukka and E. Nordlander, *Dalton Trans.*, 2008, 993–996.
27 A. K. Boudalis, R. E. Aston, S. J. Smith, R. E. Mirams, M. J. Riley, G. Schenk, A. G. Blackman, L. R. Hanton and L. R. Gahan, *Dalton Trans.*, 2007, 5132–5139.
28 J. Chen, X. Wang, Y. Zhu, J. Lin, X. Yang, Y. Li, Y. Lu and Z. Guo, *Inorg. Chem.*, 2005, **44**, 3422–3430.
29 P. Karsten, A. Neves, A. J. Bortoluzzi, M. Lanznaster and V. Drago, *Inorg. Chem.*, 2002, **41**, 4624–4626.
30 M. Lanznaster, A. Neves, A. J. Bortoluzzi, V. V. E. Aires, B. Szpoganicz, H. Terenzi, P. C. Severino, J. M. Fuller, S. C. Drew, L. R. Gahan, G. R. Hanson, M. J. Riley and G. Schenk, *JBIC, J. Biol. Inorg. Chem.*, 2005, **10**, 319–332.
31 S. J. Smith, A. Casellato, K. S. Hadler, N. Mitic, M. J. Riley, A. J. Bortoluzzi, B. Szpoganicz, G. Schenk, A. Neves and L. R. Gahan, *JBIC, J. Biol. Inorg. Chem.*, 2007, **12**, 1207–1220.
32 J. K. Bashkin, *Curr. Opin. Chem. Biol.*, 1999, **3**, 752–758.
33 A. Neves, M. Lanznaster, A. J. Bortoluzzi, R. A. Peralta, A. Casellato, E. E. Castellano, P. Herrald, M. J. Riley and G. Schenk, *J. Am. Chem. Soc.*, 2007, **129**, 7486–7487.
34 A. Neves, M. A. de Brito, V. Drago, K. Griesar and W. Haase, *Inorg. Chim. Acta*, 1995, **237**, 131–135.
35 G. Schenk, R. A. Peralta, S. C. Batista, A. J. Bortoluzzi, B. Szpoganicz, A. K. Dick, P. Herrald, G. R. Hanson, R. K. Szilagyi, M. J. Riley, L. R. Gahan and A. Neves, *JBIC, J. Biol. Inorg. Chem.*, 2008, **13**, 139–155.
36 L. L. Koh, J. O. Ranford, W. T. Robinson, J. O. Svensson, A. L. C. Tan and D. Wu, *Inorg. Chem.*, 1996, **35**, 6466–6472.
37 J. M. Botha, K. Umakoshi, Y. Sasaki and G. J. Lamprecht, *Inorg. Chem.*, 1998, **37**, 1609–1615.
38 R. T. Paine, Y.-C. Tan and X.-M. Gan, *Inorg. Chem.*, 2001, **40**, 7009–7013.
39 N. M. F. Carvalho, A. Horn Jr., R. B. Faria, A. J. Bortoluzzi, V. Drago and O. A. C. Antunes, *Inorg. Chim. Acta*, 2006, **359**, 4250–4258.
40 A. M. W. Cargill Thompson, D. A. Bardwell, J. C. Jeffery and M. D. Ward, *Inorg. Chim. Acta*, 1998, **267**, 239–247.
41 C. White, S. J. Thompson and P. M. Maitlis, *J. Organomet. Chem.*, 1977, **134**, 319–325.
42 S. Kitagawa, M. Kondo, S. Kawata, S. Wada, M. Maekawa and M. Munakata, *Inorg. Chem.*, 1995, **34**, 1455–1465.
43 U. Bossek, G. Haselhorst, S. Ross, K. Wieghardt and B. Nuber, *J. Chem. Soc., Dalton Trans.*, 1994, 2041–2048.
44 N. G. Connelly, T. Einig, G. G. Herbosa, P. M. Hopkins, C. Mealli, A. G. Orpen, G. M. Rosair and F. Viguri, *J. Chem. Soc., Dalton Trans.*, 1994, 2025–2039.
45 A. R. Sherman, in Pyridine, *Encyclopedia of Reagents for Organic Synthesis*, ed. L. A. Paquette, J. Wiley & Sons, New York, 2004.
46 G. P. Mullen, E. H. Sepersu, L. J. Ferrin, L. A. Loeb and A. S. Midvan, *J. Biol. Chem.*, 1990, **265**, 14327.
47 I. H. Segel, *Enzyme Kinetics: Behavior and Analysis of Rapid Equilibrium and Steady-State Enzyme Systems*, Wiley-Interscience, New York, 1975.
48 J. Xia, Y. Shi, Y. Zhang, Q. Miao and W. Tang, *Inorg. Chem.*, 2003, **42**, 70–77.
49 B. Bauer-Siebenlist, F. Meyer, E. Farkas, D. Vidovic, J. A. Cuesta-Seijo, R. Herbst-Irmer and H. Pritzkow, *Inorg. Chem.*, 2004, **43**, 4189–4202.
50 C. Bazzicalupi, A. Bencini, E. Berni, A. Bianchi, V. Fedi, V. Fusi, C. Giorgi, P. Paolettti and B. Valtancoli, *Inorg. Chem.*, 1999, **38**, 4115–4122.
51 A. Bencini, E. Berni, A. Bianchi, V. Fedi, C. Giorgi, P. Paolettti and B. Valtancoli, *Inorg. Chem.*, 1999, **38**, 6323–6325.
52 M. Arca, A. Bencini, E. Berni, C. Caltagrione, F. A. Devillanova, F. Isaia, A. Garau, C. Giorgi, V. Lippolis, A. Perra, L. Tei and B. Valtancoli, *Inorg. Chem.*, 2003, **42**, 6929–6939.
53 B. Bauer-Siebenlist, F. Meyer, E. Farkas, D. Vidovic and S. Dechert, *Chem.–Eur. J.*, 2005, **11**, 4349–4360.
54 E. Kimura, T. Shiota, T. Koike, M. Shiro and M. Kodama, *J. Am. Chem. Soc.*, 1990, **112**, 5805–5811.
55 T. Koike and E. Kimura, *J. Am. Chem. Soc.*, 1991, **113**, 8935–8941.
56 Y. Gultneh, A. R. Khan, D. Blaise, S. Chaudhry, B. Ahvazi, B. B. Marvey and R. J. Butcher, *J. Inorg. Biochem.*, 1999, **75**, 7–18.
57 M. Yashiro, H. Kaneiwa, K. Onaka and M. Komiyama, *Dalton Trans.*, 2004, 605–610.
58 L. M. Berreau, *Eur. J. Inorg. Chem.*, 2006, 273–283.
59 M. Livieri, F. Mancin, U. Tonellato and J. Chin, *Chem. Commun.*, 2002, 2862–2863.
60 R. Mitra, M. W. Peters and M. J. Scott, *Dalton Trans.*, 2007, 3924–3935.
61 N. V. Kaminskaia, C. He and S. J. Lippard, *Inorg. Chem.*, 2000, **39**, 3365–3373.
62 C. He and S. J. Lippard, *J. Am. Chem. Soc.*, 2000, **122**, 184–185.
63 C. R. Samples, T. Howard, F. M. Raushel and V. J. De Rose, *Biochemistry*, 2005, **44**, 11005–11013.
64 K.-Y. Wong and J. Gao, *Biochemistry*, 2007, **46**, 13352–13369.
65 G. Schenk, L. R. Gahan, L. E. Carrington, N. Mitic, M. Valizadeh, S. E. Hamilton, J. De Jersey and L. W. Guddat, *Proc. Natl. Acad. Sci. U. S. A.*, 2005, **102**, 273–278.
66 R. S. Cox, G. Schenk, N. Mitic, L. R. Gahan and A. C. Hengge, *J. Am. Chem. Soc.*, 2007, **129**, 9550–9551.
67 D. W. Christianson, *Acc. Chem. Res.*, 2005, **38**, 191–201.
68 S. Ciurli, Urease: Recent Insights on the Role of Nickel, *Metal Ions in Life Sciences*, ed. A. Sigel, H. Sigel and R. Sigel, John Wiley & Sons, Chichester, 2007.
69 S. Ciurli, S. Benini, W. R. Rypniewski, K. S. Wilson, S. Miletti and S. Mangani, *Coord. Chem. Rev.*, 1999, **190–192**, 331–355.
70 C. R. Samples, F. M. Raushel and V. J. DeRose, *Biochemistry*, 2007, **46**, 3435–3442.
71 X. Wang, R. Y. N. Ho, A. K. Whiting and L. Que Jr., *J. Am. Chem. Soc.*, 1999, **121**, 9235–9236.
72 M. B. Twitchett and A. G. Sykes, *Eur. J. Inorg. Chem.*, 1999, 2105–2115.
73 B. K. Takasaki and J. Chin, *J. Am. Chem. Soc.*, 1995, **117**, 8582–8585.
74 G. Feng, D. Natale, R. Prabaharan, J. C. Mareque-Rivas and N. H. Williams, *Angew. Chem., Int. Ed.*, 2006, **45**, 7056–7059.
75 M. Monroe, Molecular weight calculator for Windows 9x/ME/NT/00/XP, version 6.35, http://www.alchemistmatt. com.
76 A. Altomare, M. C. Burla, M. Camalli, G. L. Cascarano, C. Giacovazzo, A. Guagliardi, A. G. G. Moliterni, G. Polidori and R. Spagna, *J. Appl. Crystallogr.*, 1999, **32**, 115.
77 G. M. Sheldrick, *SHELXL-97, Program for refinement of crystal structures*, University of Göttingen, Germany, 1997.
78 L. J. Farrugia, *J. Appl. Crystallogr.*, 1999, **32**, 837–838.
79 L. J. Farrugia, *J. Appl. Crystallogr.*, 1999, **30**, 565.
80 P. Gans, A. Sabatini and A. Vacca, *J. Chem. Soc., Dalton Trans.*, 1985, 1195–1200.

